

# Bayesian estimation of acoustic emissions source in plate structures using particle filtering

Debarshi Sen, Kalil Erazo, Satish Nagarajaiah

## Abstract

In this paper a Bayesian approach for acoustic emissions source localization in plate structures is presented. The approach employs time-of-flight measurements of guided waves using triangulation to estimate the acoustic emission source in a probabilistic framework, incorporating uncertainties related to material properties, measurement noise and geometry of the system of interest. The estimate of the source location is given by a probability density function conditional on the guided wave measurements, found using a stochastic simulation algorithm known as the particle filter. The particle filter provides a non-parametric estimate of the posterior in the form of a weighted set of samples, overcoming the challenges related to the evaluation of high dimensional integrals in an efficient way. The approach is experimentally validated in a laboratory environment using an aluminum plate instrumented with three piezoelectric sensors. It is shown that the proposed approach has the capability to locate the emission source under minimal instrumentation, providing confidence intervals as a quantitative measure of the uncertainty in the estimates.

**Keywords:** Bayesian Estimation, Particle Filter, Acoustic Emissions, Source Identification, Structural Damage

## 1 Introduction

Failure of structural and mechanical systems have promoted the development of structural health monitoring (SHM) in different applications. The main tasks of SHM can be broadly classified as damage diagnosis (detection, localization and quantification) and damage prognosis (damage prediction and estimation of remaining useful life). Traditional vibration-based SHM algorithms rely on the use of dynamic response measurements to detect changes in damage-sensitive features, usually stiffness, vibration frequencies, mode shapes, among others [1]. Recently the use of ultrasonic guided waves (UGW) measurements has been a popular approach for SHM in aerospace and structural engineering applications [2, 3, 4, 5, 6]. This generally entails one of the following schemes: i) active monitoring using artificial and external high frequency excitations; ii) passive monitoring by sensing high frequency waves due to ambient processes affecting the system at hand. This paper focuses on passive approaches using UGW bypassing the need to excite the system of interest.

The objective of passive approaches using UGW is to be able to sense elastic waves propagating in the structure and localize the source of the elastic wave. This is referred to in the literature as the acoustic emission (AE) source localization problem. Acoustic emissions are UGW produced due to propagation of cracks. AE based approaches are used for source localization in systems ranging from civil structures to mechanical components and tools [7, 8]. The AE research community has actively developed efficient schemes for performing source localization; a brief review can be found in Kundu [9].

In the context of SHM applications ultrasonic waves have been employed for identifying structural damage using time-of-flight (TOF) and attenuated amplitude [10, 11, 12, 13]. The time-of-flight is defined as “the time lag from the moment when a sensor catches the damage-reflected signal to the moment when the same sensor catches the incident signal ” [14]. Various approaches are used in the literature to calculate the TOF, including thresholding procedures or envelope algorithms based on a Hilbert or Wavelet transform [11]. Algorithms developed for TOF-based source localization range in complexity from triangulation [9] to application of numerical schemes like Genetic Algorithms [15] and Neural Networks [16].

Although these algorithms have their own advantages and limitations, one inherent issue is the effect of uncertainties on the accuracy of the AE source location estimate [17]. Sources of uncertainty include variability in mechanical

properties of materials, measurement noise, and geometry of the system of interest. These uncertainties can be incorporated in the analysis by adopting a probabilistic model. In particular Bayesian inference can be adopted as a consistent and rigorous theory that can be applied for a large class of estimation problems [18, 19]. In Bayesian inference the unknown quantities are modeled as random variables, and their estimate is given by a probability density function (PDF) conditional on the available data, obtained in principle using Bayes' theorem. When using complex nonlinear models, the functions needed to evaluate the posterior are difficult to obtain in closed-form.

In this paper a Bayesian approach is proposed to estimate acoustic emission sources in plate type structures. For this purpose a particle filter is employed to obtain a non-parametric estimate of the source posterior probability density function. The particle filter is a stochastic simulation algorithm that uses a set of samples to approximate the posterior probability density function as a probability mass function (PMF) that converges to the former as the number of samples increases [20]. Particle filters were originally developed for recursive estimation of dynamic systems [21], but can also be adapted for static problems as discussed in a further section of this paper. An advantage of the proposed approach is that it imposes no restriction on the functional form of the prior distribution, allowing to use any probability density function. Of particular interest is to use a non-informative prior in order to maximize the weight of the data (Bayesian data-driven) [18].

The proposed approach is experimentally validated in a laboratory environment using an aluminum plate. A pencil lead break on the plate surface is used to simulate an acoustic emission source (also known as the Hsu-Nielsen source [22]). It is shown that the proposed approach has the capability to locate the source correctly, with the minimum number of sensors necessary for triangulation, providing confidence intervals describing the uncertainty in the estimated source location.

## 2 Acoustic Emissions Source Localization

The premise behind acoustic emission source localization is that elastic waves are generated when a structure is impacted by foreign bodies or a crack propagation is initiated in a system. If multiple sensors acquire the elastic wave signals, the time-of-flight (TOF) of the waves can be used to estimate the location (in a Cartesian coordinate system) of the source generating them, in a similar way as the location of the epicenter of an earthquake is estimated using a triangulation scheme. When the velocity of the propagating wave is known *a priori*, the distance from the source to the corresponding receiver is estimated from the TOF data as discussed below. Although several approaches for source location estimation have been explored in the literature, the TOF-based triangulation still remains a popular choice owing to its simplicity and accuracy.

In a deterministic setting the geometric and material properties of the system, and the TOF measurement are assumed to be perfectly known. The group velocity of acoustic waves ( $V_g$ ) is obtained from dispersion curves of Lamb waves (the thickness of the plate is assumed to be small enough such that it is amenable for generation of Lamb Waves). If the TOF from sensor  $i$  is  $t_i$ , the following relationship is used to relate the source location to the TOF

$$t_i = \frac{1}{V_g} \sqrt{(x_i - x_S)^2 + (y_i - y_S)^2} \quad i = 1, 2, \dots, n \quad (1)$$

where the coordinates  $(x_i, y_i)$  and  $(x_S, y_S)$  are, respectively, the Cartesian coordinates of sensor  $i$  and the acoustic emission source. The total number of available sensors is  $n$ . The geometric interpretation of this approach is to simply draw circles of radius  $r_i = V_g t_i$  around each sensor, and to find the point of intersection of these circles. This is shown schematically in Figure 1.

A drawback of this (deterministic) approach is that it does not incorporate sources of uncertainty, such as material properties of the plate, the frequency content of the load applied and the noise in measurements. All these uncertainties collude and lead to a situation shown in Figure 1. The bands of color show the uncertainty that propagates to the estimated acoustic source location. In the Bayesian probabilistic approach discussed in a following section, the AE source location and the wave propagation velocity are treated as random variables described by a probability distribution that incorporates the uncertainties involved.

Although recent research in the subject has considered some of the sources of uncertainty, the inverse problem of finding the source location with only three sensors (which is the minimum number of sensors required for triangulation on a 2-D plane) has proven to be a challenging task [17]. Clearly, a large number of sensors will effectively reduce the

effects of uncertainties on the performance of any algorithm. However, it is of interest to be able to restrict the number of sensors to a minimum. This is important to reduce economic costs of the monitoring system, and also because the number and location of the sensors might be restricted by the physical configuration of the system. The estimation of the TOF is discussed in the following section.

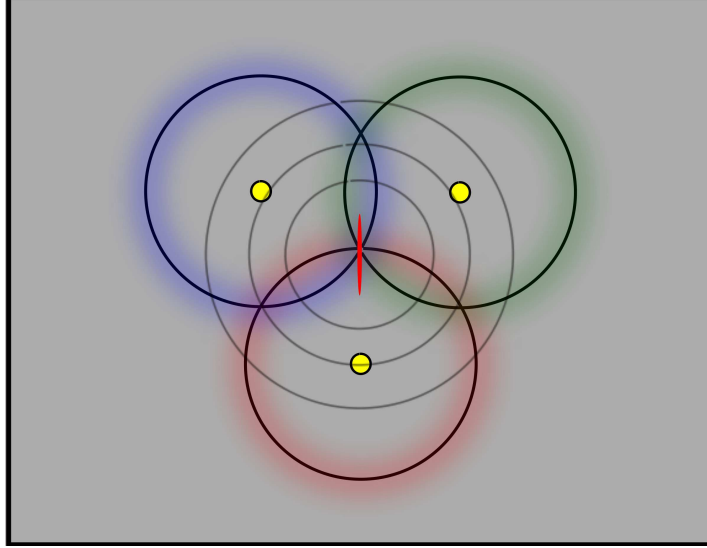


Figure 1: Source estimation from triangulation. The yellow disks denote the sensors, the red patch is the source (in this case structural damage in the form of a crack), the gray circles are the AE waves propagating outward from the damage, the black circles along with the blurred colors are the circles with radius obtained from TOF data along with the associated uncertainties.

### 3 Wavelet Transform based Time of Flight Estimation

To estimate the location of AE sources wave travel time measurements are needed. In this paper a continuous wavelet transform (CWT) is performed on the signals to isolate the primary frequency and estimate the time of arrival of that content. The use of CWT is justified by its efficacy in time frequency analysis of signals. Although other time-frequency decomposition methods like short time Fourier transform (STFT) or Hilbert-Huang transform (HT) may suffice for TOF estimation, the frequency content information is also critical in the proposed algorithm. The algorithm not only takes into account the uncertainties in the AE source location, but also the uncertainty involved in the group velocity.

An initial estimate of the group wave velocity is obtained using the frequency content of the signal and the dispersion curves. The specific wavelet used for this task is the complex Morlet wavelet, which is defined by

$$f(x) = \frac{1}{\sqrt{\pi f_b}} \exp(i2\pi f_c x - x^2/f_b) \quad (2)$$

where,  $f_b$  and  $f_c$  are the frequency bandwidth and the central frequency respectively. A typical complex Morlet Wavelet is shown in Figure 2. Figure 3 shows a typical response signal acquired from the experimental setup used in the paper (details of the setup are discussed later). The CWT of the signal is shown in Figure 4. As it can be seen, wavelet level 43 contains the majority of the frequency content of the signal. The arrival of the peak frequency at level 43 is hence treated as the TOF. The initial estimate obtained by this approach will be employed to define a prior distribution for Bayesian estimation. This is further discussed in the following section.

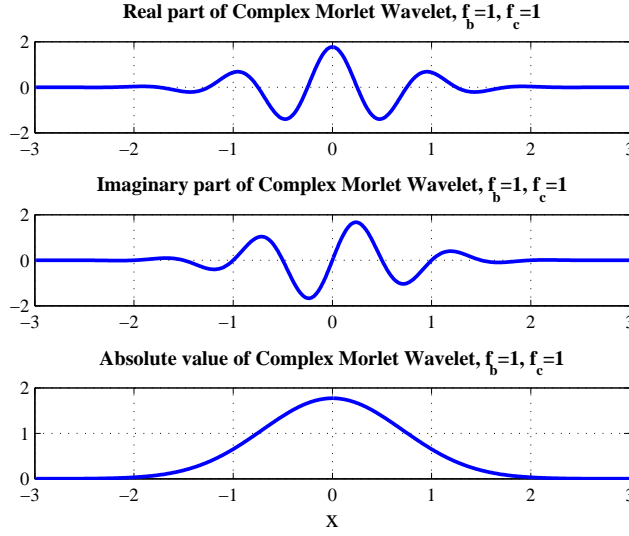


Figure 2: Absolute value, Real and Imaginary parts of the complex Morlet wavelet with  $f_b = 1$  and  $f_c = 1$

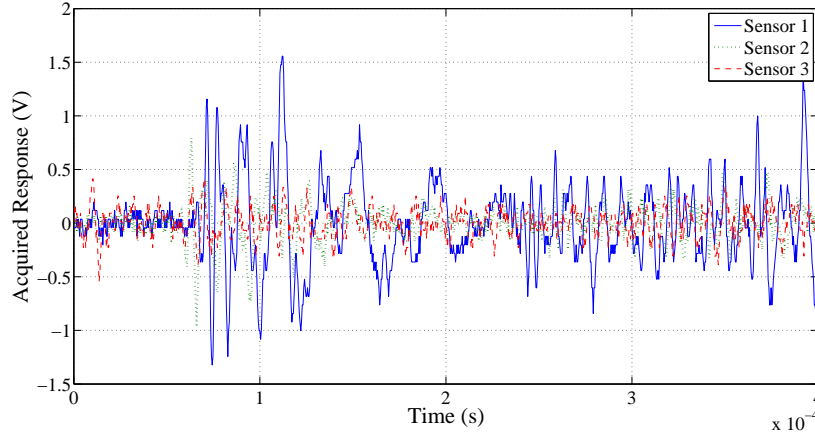


Figure 3: A typical set of signals acquired from AE experiments on a square aluminum plate (edge length 91 cm) from three sensors. Details of the experimental setup has been discussed later and can be found in Figure 7

## 4 Bayesian Parameter Estimation

In Bayesian estimation the parameters to be estimated,  $\Phi \in \mathbb{R}^n$ , are treated as random variables, and their estimate is given by a probability density function (PDF) conditional on the available information. The estimated PDF (also known as the posterior PDF) is denoted as  $p(\Phi|\mathbf{Y})$  where  $\mathbf{Y}$  is the gathered data. In principle, the posterior is given by Bayes' theorem

$$p(\Phi|\mathbf{Y}) = \frac{p(\mathbf{Y}|\Phi)p(\Phi)}{p(\mathbf{Y})} \quad (3)$$

where  $p(\Phi)$  denotes the prior distribution,  $p(\mathbf{Y}|\Phi)$  as a function of  $\Phi$  is the likelihood function, and  $p(\mathbf{Y})$  is a normalizing constant. The prior distribution  $p(\Phi)$  is used to incorporate information available about the parameters before the data is available. Since in our application the location of the emissions source is unknown, it is desired to reduce the weight of the prior in the estimation as much as possible. For example, the use of a Gaussian distribution for

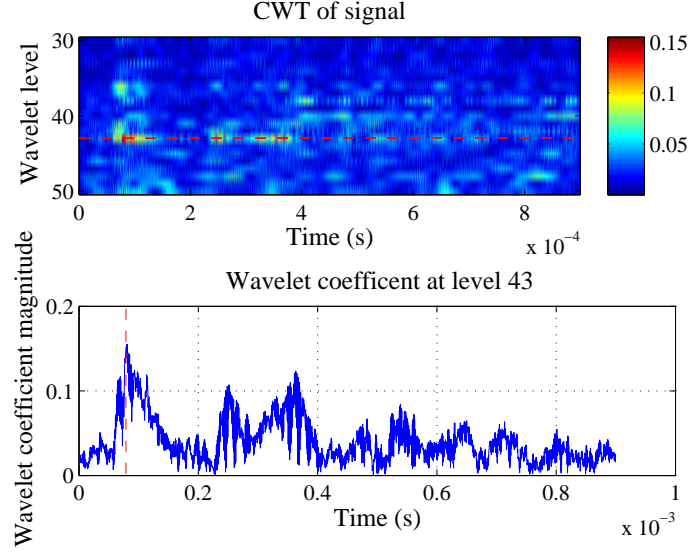


Figure 4: CWT of signal from Sensor 1 in Figure 3. The dominant frequency level is marked by the horizontal red dashed line. The TOF can be estimated by the arrival time of this dominant frequency as shown by the vertical red dashed line

the prior induces a strong bias, requiring an increased amount of information (data) to shift the prior mean towards the source location. For this reason in this paper we will adopt a non-informative prior such that its effect in the posterior is minimized, resulting in a Bayesian data-driven approach where the information contained in the data is maximized [18].

From the posterior distribution a point value can be selected (usually the mean or the mode). The mode of the posterior (or maximum a posteriori estimate) is

$$\Phi_{MAP} = \arg \max_{\Phi} p(\Phi|\mathbf{Y}) \quad (4)$$

The marginal distributions of parameter  $\Phi_i$  are also of interest, and given by

$$p(\Phi_i|\mathbf{Y}) = \int p(\Phi|\mathbf{Y})d(\Phi \setminus \Phi_i) \quad (5)$$

where the integral is about a measure that excludes the subspace of  $\Phi_i$  ( $\Phi \setminus \Phi_i$  denotes a set where subspace  $\Phi_i$  is excluded from set  $\Phi$ ). To quantify the uncertainty in the estimates confidence intervals (CI) are used. Bayesian confidence intervals provide the probability that the true parameter lies in a region of the parameter space, given the observed data. For parameter  $\Phi_i$  the CI is defined as

$$CI_i = [\phi_i^a, \phi_i^b] \quad \text{such that} \quad P(\Phi_i \in CI_i|\mathbf{Y}) = \int_{\phi_i^a}^{\phi_i^b} p(\Phi_i|\mathbf{Y})d\Phi_i \quad (6)$$

where  $P(\Phi_i \in CI_i|\mathbf{Y})$  is a target probability. In practice the 95% mode-centered confidence interval is typically employed. To formulate the emission source estimation problem in the Bayesian probabilistic setting the residual error vector is defined as

$$e(\Phi) = \mathbf{Y} - \hat{\mathbf{Y}}(\Phi) = \mathbf{Y} - h(\Phi) \quad (7)$$

where  $\hat{\mathbf{Y}}(\Phi)$  is the estimate of the response (time of flight), obtained using the mapping  $h$  defined by Eq. 1. The residual vector is the estimation error resulting mainly from modeling errors and measurement noise. The residual is generally modeled as a white noise sequence, and when only a mean vector and covariance matrix are available, a

Gaussian distribution yields the maximum entropy distribution [19]. Under such conditions the likelihood function is given by

$$p(\mathbf{Y}|\Phi) = \frac{1}{\sqrt{(2\pi)^n |\mathbf{R}|}} e^{-\frac{1}{2}(\mathbf{Y}-h(\Phi))^T \mathbf{R}^{-1}(\mathbf{Y}-h(\Phi))} \quad (8)$$

where  $|\mathbf{R}|$  is the determinant of  $\mathbf{R}$ , and the posterior becomes

$$p(\Phi|\mathbf{Y}) = \frac{p(\Phi)}{p(\mathbf{Y})} \frac{1}{\sqrt{(2\pi)^n |\mathbf{R}|}} e^{-\frac{1}{2}(\mathbf{Y}-h(\Phi))^T \mathbf{R}^{-1}(\mathbf{Y}-h(\Phi))} \quad (9)$$

Although straightforward in principle, the estimation poses significant implementation, numerical and practical difficulties, mainly because in general the posterior PDF  $p(\Phi|\mathbf{Y})$  cannot be computed in closed-form, especially when nonlinear models are used [18]. For instance, the computation of the normalization factor  $p(\mathbf{Y})$  involves a multidimensional integral over the parameter space, which cannot be computed in closed-form in general. Moreover, to obtain the marginal distributions of the parameters similar integrals over subspaces of the parameter space are required.

Under special conditions, such as when the number of measurements or data is large, asymptotic (Laplace) approximations may be employed. The asymptotic posterior approaches a Gaussian distribution in the limit of increasing data, a result known as Bernstein-Von Mises theorem [18]. A popular alternative that has gained attention in recent time is a family of methods known as Markov chain Monte Carlo (MCMC) simulation, where a sample of the posterior is obtained by constructing a Markov chain with certain asymptotic properties [23]. Specifically, a Markov chain that converges to the posterior as the limit of samples increases is constructed to explore the parameter space. The points in the chain are then treated as samples from the posterior, used to compute sampling estimates of the parameters of interest. MCMC allows to overcome the issues related to computing the integrals, at the expense of a high computational cost.

In our application to acoustic emissions source localization, we are interested in cases where the number of measurements is limited, and thus the asymptotic results cannot be adopted. Moreover, in structural health monitoring applications an efficient approach where the computational cost is minimum is needed in order to evaluate the state of damage of engineering systems in a timely manner. To overcome these difficulties the use of a stochastic simulation algorithm known as the particle filter is proposed. The particle filter is employed to obtain a set of samples as a non-parametric estimate of  $p(\Phi|\mathbf{Y})$  in the form of a probability mass function. The advantage of the non-parametric estimate is that no assumptions regarding the functional form of the prior (e.g., the typically used Gaussian distribution) or the posterior are made. The particle filter is discussed in the following section, followed by its application to the acoustic emission source localization problem.

## 5 Particle Filter

The particle filter (PF) is a Bayesian filtering algorithm used to obtain a discrete approximation to the joint probability distribution of a state-space model conditioned on response measurements [20]. The PF is suitable for applications where a Gaussian approximation cannot represent the conditional distribution accurately resulting in errors in the estimates and/or divergence of the filter; this can potentially arise when the distributions involved are multi-modal, skewed, or have heavy tails. To estimate the source location using a particle filter a state-space model needs to be defined. This state-space model constitutes only time-invariant parameters, namely the Cartesian coordinates of the source and the group wave velocity. Hence, defining the parameter state as  $\theta = \{x_S, y_S, V_g\}$ , a time-invariant state-model is given by

$$\theta_{k+1} = \theta_k \quad (10)$$

The objective is to compute the posterior PDF of the state,  $p(\theta_k|\mathbf{Y}_k)$ , as the data is gathered. The posterior is given by

$$p(\theta_k|\mathbf{Y}_k) = \frac{p(y_k|\theta_k)p(\theta_k|\mathbf{Y}_{k-1})}{p(y_k|\mathbf{Y}_{k-1})} \quad (11)$$

where  $p(y_k|\theta_k)$  is obtained from the measurements model Eq. 1, with an additive measurement noise model. In the particle filter  $p(\theta_k|\mathbf{Y}_k)$  is approximated by a discrete set of samples  $\{\theta_k^i\}$  as

$$\hat{p}(\theta_k|\mathbf{Y}_k) = \frac{1}{N} \sum_{i=1}^N \delta_{\theta_k^i}(\theta_k) \quad (12)$$

where  $\delta_{\theta_0}(\theta)$  is the Dirac measure at  $\theta_0$ . Statistical moments of  $p(\theta_k|\mathbf{Y}_k)$  are then readily estimated from the sample. Since  $p(\theta_k|\mathbf{Y}_k)$  is unknown (and thus cannot be directly sampled), an importance sampling strategy is typically employed.

In order to arrive to a recursive implementation (i.e., a method where samples from previous steps are used in the current step) an alternative formulation is useful. Let  $\Theta_k$  denote the set of states  $\Theta_k = \{\theta_0, \theta_1, \dots, \theta_k\}$ , then from Bayes theorem and using the structure of the output and dynamic models, it follows that [21]

$$p(\Theta_k|\mathbf{Y}_k) = \frac{p(\theta_0)}{p(\mathbf{Y}_k)} \prod_{i=1}^k p(y_i|\theta_i) p(\theta_i|\theta_{i-1}) \quad (13)$$

To obtain features of the joint posterior distribution in Eq. 13, such as marginal distributions, high-dimensional integrals need to be evaluated. Moreover, the distribution of the data  $p(\mathbf{Y}_k)$  typically cannot be computed analytically. An alternative is to recur to stochastic simulation, where samples are used to represent and evolve the probability distributions on time [20].

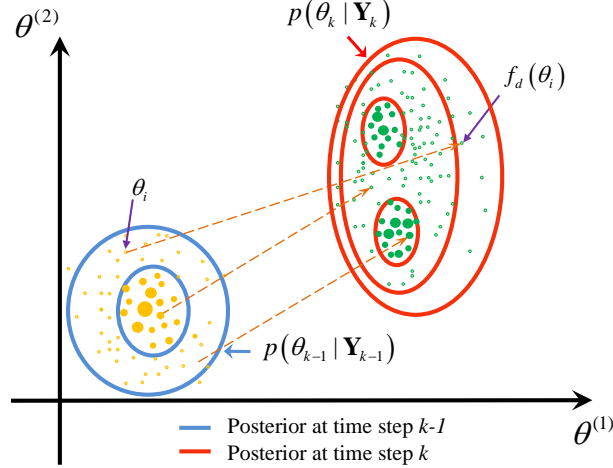


Figure 5: Particle filter. A set of weighted samples is used to approximate a conditional probability density function by a probability mass function.

The traditional approach used to obtain a recursive algorithm is based in importance sampling (IS), originally a Monte-Carlo integration method. With IS expectations of functions of the state given by

$$\mathbb{E}[g(\Theta_k)] = \int g(\Theta_k) p(\Theta_k|\mathbf{Y}_k) d\Theta_k \quad (14)$$

are estimated as

$$\hat{\mathbb{E}}[g(\Theta_k)] = \sum_{i=1}^N g(\Theta_k^{(i)}) \tilde{w}_n^{(i)} \quad (15)$$

$$\tilde{w}_n^{(i)} = \frac{w_n^{(i)}}{\sum_{j=1}^N w_n^{(j)}} \quad w_n^{(i)} = \frac{p(\mathbf{Y}_k|\Theta_k^{(i)}) p(\Theta_k^{(i)})}{\pi(\Theta_k^{(i)}|\mathbf{Y}_k)} \quad (16)$$

where,  $\{\Theta_k^{(i)}\}_{i=1}^N$  is a set of independent samples drawn from the importance distribution  $\pi(\cdot)$ . In this formulation the distribution of the data  $p(\mathbf{Y}_k)$  is also estimated using  $\pi(\cdot)$ , so that it does not have to be computed analytically. If the support of  $\pi(\cdot)$  includes the support of  $p(\Theta_k|\mathbf{Y}_k)$  and  $\mathbb{E}[g(\Theta_k)]$  is finite, the estimator  $\widehat{\mathbb{E}}[g(\Theta_k)]$  converges almost surely to  $\mathbb{E}[g(\Theta_k)]$ , and the rate of convergence depends on the choice of  $\pi(\cdot)$  [20]. When a recursive algorithm is desired, the typical choice is a function of the form [21]

$$\pi(\Theta_k|\mathbf{Y}_k) = \pi(\theta_0) \prod_{i=0}^k \pi(\theta_i|\Theta_{i-1}, \mathbf{Y}_i) \quad (17)$$

and a convenient choice for the marginal proposals is the transition PDF of the model  $\pi(x_i|\Theta_{i-1}, \mathbf{Y}_i) = p(\theta_i|\theta_{i-1})$ ; it follows that the weights can be calculated recursively as

$$w_k^{(i)} = w_{k-1}^{(i)} p(y_k|\theta_k^{(i)}) \quad (18)$$

Using the updated weights the probability mass function approximating the posterior is given by

$$\widehat{p}(\theta_k|\mathbf{Y}_k) = \sum_{i=1}^N w_k^{(i)} \delta_{\theta_k^{(i)}}(\theta_k) \quad (19)$$

This approach is illustrated in Figure 5, which shows the updating of a prior distribution using the above discussed approach.

## 6 Particle Filtering Acoustic Emission Source Identification Algorithm

The algorithm resulting from employing the particle filter to estimate the acoustic emissions source location is given as follows:

- Acquire AE signals using available sensors
- Apply CWT to the acquired signals and compute the (noise contaminated) TOF data  $y = \{t_i\}$
- Based on the available information select the parameters prior distribution  $p(\Phi)$
- Select the number of samples  $N$  and set the initial weights to  $w_0^{(i)} = 1/N$
- Obtain  $N$  random samples  $\phi_i$  from the prior distribution

For  $i = 1$  to  $N$

- For each sample  $\phi_i$  estimate the time of flights  $\{\hat{t}_i\}$  using Eq. 1
- Using a Gaussian noise model the updated weights (Eq. 18) are given by  $w_1^{(i)} = w_0^{(i)} N(y, \hat{t}_i, r)$   
( $r$  is the measurement noise standard deviation)  
 $N(z, \mu, \sigma)$  is a Gaussian distribution evaluated at  $z$ , with mean  $\mu$  and standard deviation  $\sigma$

A flowchart describing the proposed algorithm is shown in Figure 6.

## 7 Experimental Validation

In this section results from an experimental validation study of the proposed approach for AE source localization using particle filtering are presented. For this purpose an aluminum plate was subjected to pencil lead break at different locations. The pencil lead break or the Hsu-Nielsen source simulates waves produced by AE sources [22]. The experimental setup consisted of a 3.51 cm thick aluminum square plate of side 91 cm. Three piezosensors were used



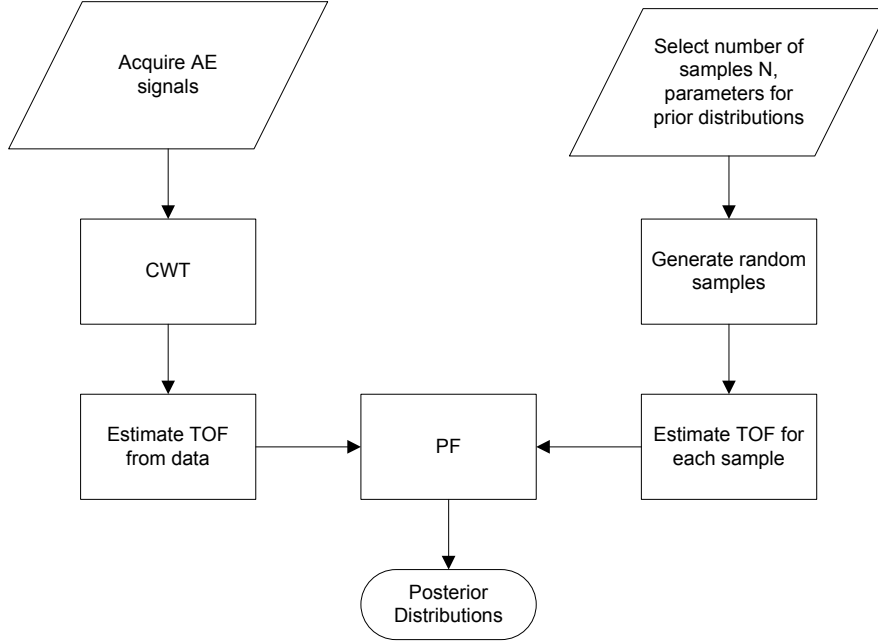


Figure 6: Flowchart showing the proposed Particle Filtering based source identification algorithm

to record the signals of the traveling waves (this is the minimum number of sensors needed for triangulation). As discussed earlier, the inverse problem of source localization using three sensors only, with parameter uncertainties incorporated has proven to be a challenging task [17]. The Piezosensors used are 10mm diameter and 3mm thick Lead Zirconate Titanate (PZT) sensors with a dominant R mode vibration at a resonant frequency of 215kHz. The sensors were attached on the plate with 3M transparent double sided tape. The signals generated at the PZT sensors are amplified and acquired through an oscilloscope TDS 2024C at a sampling rate of 10 MHz.

The experimental setup is depicted in Figure 7, where the position of the sensors are shown. The locations of the three sensors used are summarized in Table 1. The green crosses on the plate, along with the corresponding numbers, are the different simulated AE sources used for the experiment. The locations of all the possible AE sources are listed in Table 2. Six different locations of the AE source were used.

As discussed earlier, the vector of parameters to be estimated is  $\theta = \{x_S, y_S, V_g\}$ . The prior distribution of the source location was selected as a uniform (“flat”) two dimensional distribution covering the plate. The use of this non-informative distribution is one of the main features of the proposed approach, since it allows the data to control the posterior. A Gaussian prior, on the other hand, would have attributed higher weights to coordinates in the vicinity of the prior mean, hence, imposing a significant bias in the estimate.

To highlight this feature the performance of the proposed algorithm will be compared to an unscented Kalman filter (UKF) based algorithm, where Gaussian prior and posteriors for the AE source coordinates are used [17]. This is the basis for dividing the plate into two different regions as shown in Figure 7. The region inside the red rectangle is where the actual AE source is in the vicinity of the prior mean of the source coordinates. Hence, inside this region, the UKF based algorithm might still perform satisfactorily as the likelihood distribution will be high due to a large pre-assigned weight, owing to the shape of a Gaussian distribution. For points further away the results will be affected as the information contained in the minimum number of sensors used (three sensors) is not enough to overcome the strong bias in the prior. It should be pointed out that effect of the prior bias is alleviated by increasing the number of sensors, however, for practical considerations it is desired to keep the number of sensors at a minimum. The estimation accuracy of the unscented Kalman filter and the particle filter has been assessed in validation studies, where it has been shown that under limited instrumentation and increased nonlinearity the PF outperforms the UKF [24, 25].

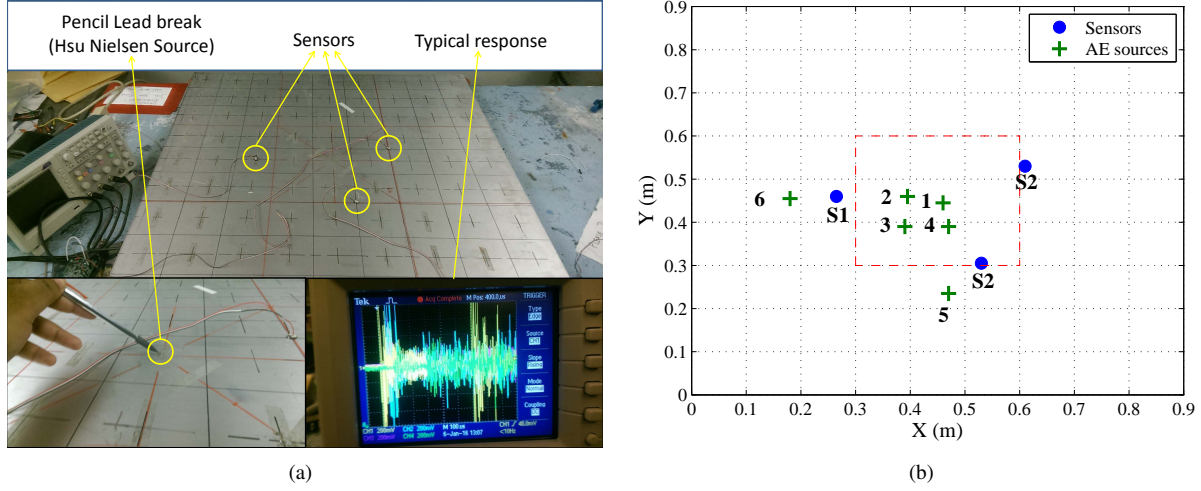


Figure 7: Experimental setup showing the location of the sensors and the location of the AE sources.

Due to the uncertainty in the group velocity, the frequency content of signals acquired at each sensor was used in conjunction with available dispersion curves for Lamb waves for selecting the mean of the prior for the group velocity. Due to the existing dispersion curves, and lower uncertainties associated with material properties, a Gaussian prior is effective in capturing the uncertainties involved in group velocities.

In the proposed particle filtering based approach, the prior distributions for the source coordinates are uniformly sampled. The prior distribution for the group wave velocity was selected as a Gaussian distribution with mean  $\mu_{V_g} = 2600\text{m/s}$  and a coefficient of variation of 10%. The joint distributions are then updated using weights that reflect how well the samples reproduce the measurements. In this example 30,000 random samples of the prior were used. The prior distribution for the coordinates are depicted in Figure 8(a). Figure 8(b) shows a typical randomly drawn sample for the coordinates using the PF algorithm, which was used to construct the posterior probability density function, with the diameter of each point representative of the associated weight assigned by the algorithm.

Figure 9 shows the posterior distributions obtained for two different locations, 1 and 5 as described in Figure 7. As can be seen in Figures 9(a) and (c), the estimates obtained are in agreement with the actual source locations. Moreover, the distribution is highly peaked, and thus the uncertainty in the estimates is small. The posterior distribution of the group wave velocity is also depicted in this figure. Figure 9(b) and Figure 9(d) shows the prior and the posterior distribution of the wave group velocity.

The estimation results are summarized in Table 3, where the 95% mean-centered confidence intervals (C.I.) are shown as a quantitative measure of the uncertainty in the parameters. In terms of computational cost the proposed approach is very efficient, taking only a few seconds to run the algorithm on a desktop computer. As mentioned before, the efficiency of stochastic simulation algorithms is of importance for practical applications, such as structural health monitoring applications where a decision about the state of damage of an engineering system needs to be taken in a short period of time after a potentially damaging event.

The performance of the algorithm was compared to the previously proposed UKF-based scheme, with the prior mean located at the center of the plate [17]. Figure 10 compares the results from the UKF-based and the proposed PF-based approaches. As can be seen the performance of the UKF-based approach decreases as the source location moves away from the center of the plate. In order to assess the results quantitatively the following relative  $\ell_2$  error norm was defined as an error metric

$$PM = \frac{\|\hat{\mathbf{x}} - \mathbf{x}_S\|_2}{\|\mathbf{x}_S\|_2} \quad (20)$$

where  $\hat{\mathbf{x}}$  is the estimated AE source  $(\hat{x}_S, \hat{y}_S)$ ,  $\mathbf{x}_S$  is the actual AE source coordinates  $(x_S, y_S)$ , and  $\|\cdot\|_2$  denotes the  $\ell_2$  norm. The error metric results are presented in Table 4.

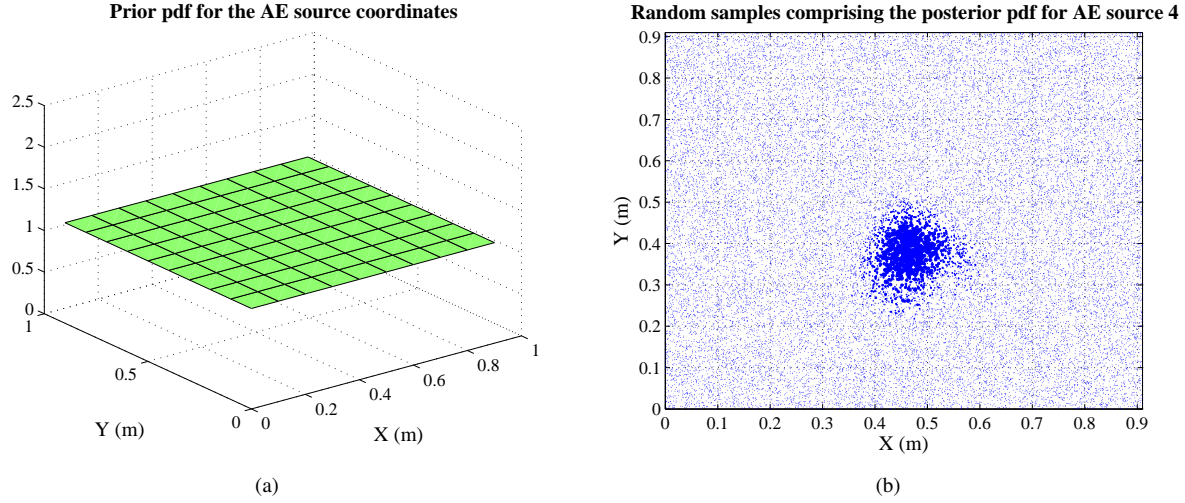


Figure 8: Prior and Posterior distributions for the coordinates. (a) Uniform PDF used as prior. (b) Posterior PDF sample; the size of each point is representative of the associated weight assigned to it by the PF.

## 8 Conclusion

A Bayesian approach for acoustic emissions source localization was presented. The approach relies on a wavelet-based time-of-flight measurements triangulation model, combined with a stochastic simulation algorithm known as the particle filter to estimate the source location. In the proposed approach a particle filter is used to obtain a non-parametric estimate of the posterior probability density function of the emissions source, incorporating in the analysis inherent uncertainties resulting from measurement noise, geometry and modeling errors.

The use of a non-parametric sampling based approach to estimate the posterior distribution allows to employ any prior distribution for the estimation. In particular a non-informative prior was adopted, eliminating the bias in the source location when there is no information available about the source location. Minimizing the effect of the prior results in a Bayesian data-driven approach where the estimate is obtained by putting most of the weight in the data.

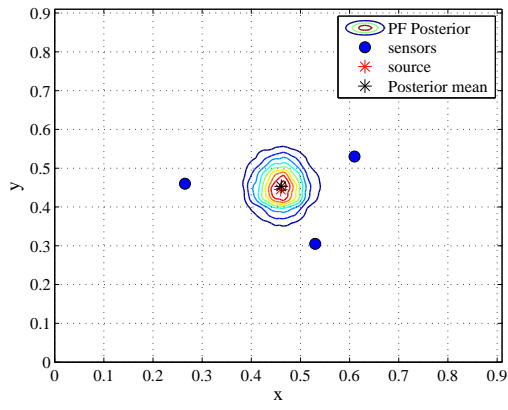
The proposed approach was experimentally validated in a laboratory environment. For this purpose an aluminum plate was subjected to pencil lead break at different locations. It was shown that the proposed algorithm has the capability to estimate the acoustic emission source accurately, with the minimum number of sensors needed for triangulation (three sensors). In addition to point estimates, confidence intervals were used to describe the uncertainty in the source location estimate. For all the cases considered the actual source location was close the posterior distribution mode, and based on the tight confidence intervals obtained the uncertainty in the estimates was small. The approach proved to be efficient in terms of the computational cost. This is desirable in structural health monitoring applications, where an estimate of the state of damage of a system needs to be provided in a timely manner after a potentially damaging event takes place.

## 9 Acknowledgment

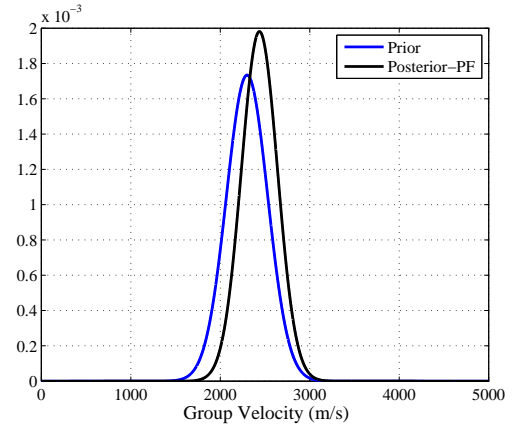
Funding by Texas Instruments for this project is gratefully acknowledged.

## References

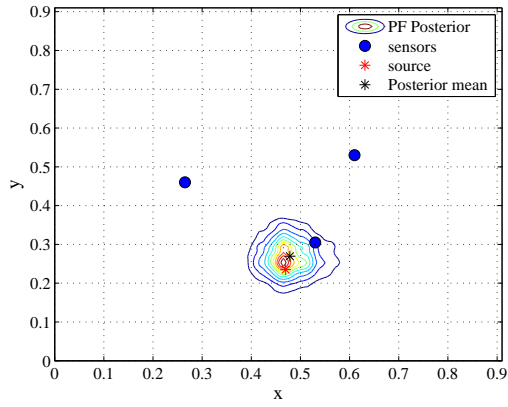
- [1] CR Farrar, S.W. Doebling, and D.A. Nix. Vibration-based structural damage identification. *Philosophical Transactions of the Royal Society of London*, 359:131–149, 2001.



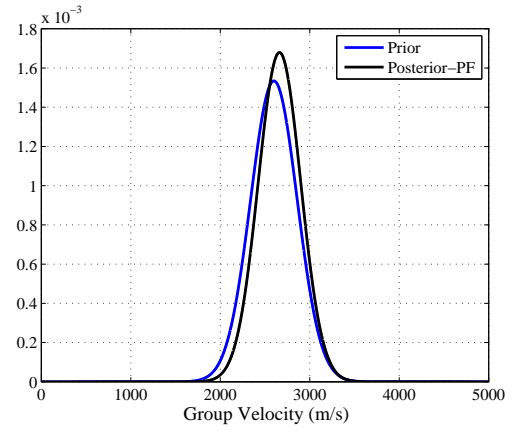
(a)



(b)



(c)



(d)

Figure 9: Posterior Distributions of the coordinates and the group velocity obtained by the proposed algorithm. Figures (a) and (b) are for location 1 and (c) and (d) are for location 5

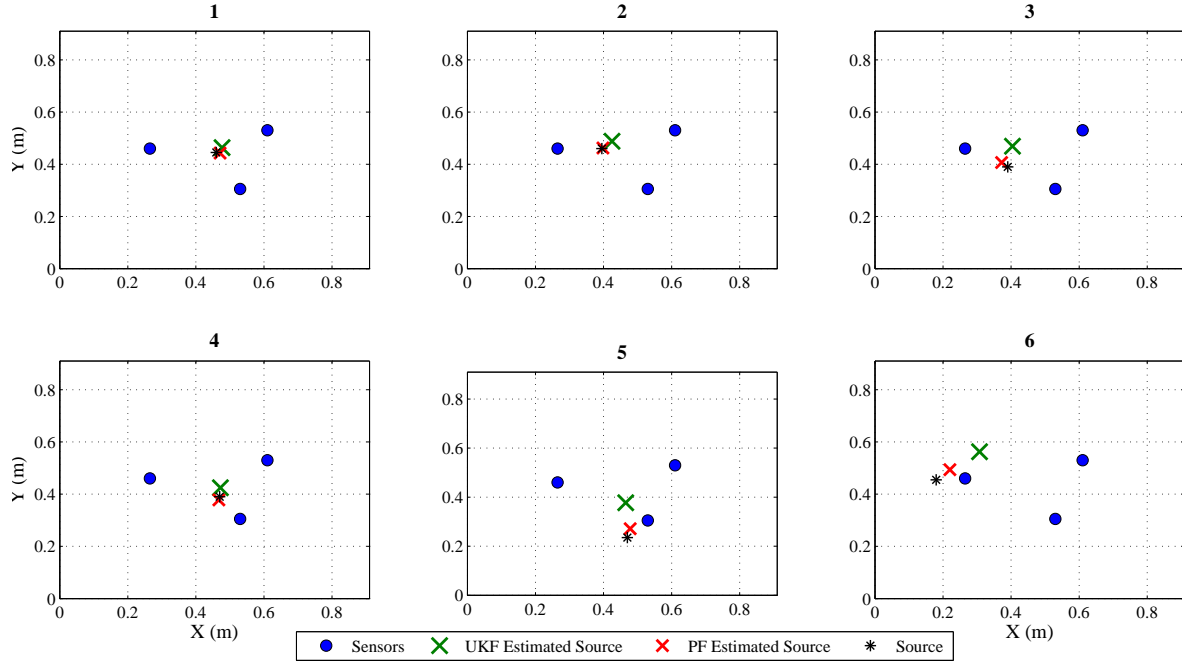


Figure 10: Comparison of UKF based algorithm and proposed PF based algorithm for different AE source locations. It can be clearly observed that the proposed algorithm outperforms the UKF based Bayesian approach.

- [2] AJ Croxford, PD Wilcox, BW Drinkwater, and G Konstantinidis. Strategies for guided-wave structural health monitoring. *Proceedings of the Royal Society A*, 463:2961–2981, 2007.
- [3] V Giurgiutiu and A Cuc. Embedded non-destructive evaluation for structural health monitoring, damage detection, and failure prevention. *The Shock and Vibration Digest*, 37(2):83–105, 2005.
- [4] JL Rose. Ultrasonic guided waves in structural health monitoring. *Key Engineering Materials*, 270-273(2):14–21, 2004.
- [5] JL Rose. A baseline vision of ultrasonic guided waves inspection potential. *Journal of Pressure Vessel Technology*, 124:273–282, 2002.
- [6] M Beard, M Lowe, and P Cawley. Embedded non-destructive evaluation for structural health monitoring, damage detection, and failure prevention. *The Shock and Vibration Digest*, 37(2):83–105, 2005.
- [7] X Li. A brief review: acoustic emission method for tool wear monitoring during turning. *International Journal of Machine Tools and Manufacture*, 42(2):157–165, 2002.
- [8] A Nair and CS Cai. Acoustic emission monitoring of bridges: Reviews and case studies. *Engineering Structures*, 32(6):1704–1714, 2010.
- [9] T Kundu. Acoustic source localization. *Ultrasonics*, 54:25–38, 2014.
- [10] S Kessler, S Spearing, and C Soutis. Damage detection in composite materials using Lamb wave methods. *Smart Materials and Structures*, 11:269–278, 2002.
- [11] BC Lee and WJ Staszewski. Lamb wave propagation modelling for damage detection: II. damage monitoring strategy. *Smart Materials and Structures*, 16:260–274, 2007.

- [12] H Sohn and CR Farrar. Damage diagnosis using time series analysis of vibration signals. *Smart Materials and Structures*, 10:1–6, 2001.
- [13] J Grabowska, M Palacz, and M Krawczuk. Damage identification by wavelet analysis. *Mechanical Systems and Signal Processing*, 22:1623–1635, 2008.
- [14] Z Su, L Ye, and Y Lu. Guided Lamb waves for identification of damage in composite structures: A review. *Journal of Sound and Vibration*, 295:753–780, 2006.
- [15] PT Coverley and WJ Staszewski. Impact damage location in composite structures using optimized sensor triangulation procedure. *Smart Materials and Structures*, 12(5):795–803, 2003.
- [16] T Fu, Z Zhang, Y Liu, and J Leng. Development of an artificial neural network for source localization using a fiber optic acoustic sensor array. *Structural Health Monitoring*, 14(2):168–177, 2015.
- [17] E Dehghan Niri and S Salamone. A probabilistic framework for acoustic emission source localization in plate like structures. *Smart Materials and Structures*, 21(035009):16, 2012.
- [18] A Gelman, J Carlin, H Stern, and D Rubin. *Bayesian Data Analysis*. Chapman and Hall CRC, Boca Raton, Florida, USA, 2004.
- [19] J Beck. Bayesian system identification based on probability logic. *Structural Control and Health Monitoring*, 17:825–847, 2010.
- [20] A Doucet, S Godsill, and C Andrieu. On sequential Monte Carlo sampling methods for Bayesian filtering. *Statistics and Computing*, 10:197–208, 2000.
- [21] J Ching, J Beck, K Porter, and R Shaikhutdinov. Bayesian state estimation method for nonlinear systems and its application to recorded seismic response. *Journal of Engineering Mechanics*, 132(4):396–410, 2006.
- [22] MGR Sause. Investigation of pencil-lead breaks as acoustic emission sources. *Journal of Acoustic Emission*, 29:184–196, 2011.
- [23] J Beck and S-K Au. Bayesian updating of structural models and reliability using Markov chain Monte Carlo simulation. *Journal of Engineering Mechanics*, 128(4):380–391, 2002.
- [24] K Erazo and E Hernandez. Uncertainty quantification of state estimation in nonlinear structural systems with application to seismic response in buildings. *ASCE/ASME Journal of Risk and Uncertainty in Engineering Systems*, B5015001, 2015.
- [25] K Erazo and E Hernandez. State estimation in nonlinear structural systems. *Nonlinear Dynamics. Proceedings of the 32nd IMAC, A Conference and Exposition on Structural Dynamics*, 2:249–257, 2014.

<b>Sensor</b>	<b>X (m)</b>	<b>Y (m)</b>
1	0.265	0.46
2	0.53	0.305
3	0.61	0.53

Table 1: Locations of PZT sensors on the plate

<b>AE Source</b>	<b>X (m)</b>	<b>Y (m)</b>
1	0.46	0.445
2	0.395	0.46
3	0.39	0.39
4	0.47	0.39
5	0.47	0.235
6	0.18	0.455

Table 2: AE source locations on the experimental plate along with the corresponding labels



	AE Source	Actual	Estimate (mean)	95% C.I.
$x$ -coordinate	1	0.46	0.47	[0.40, 0.54]
$y$ -coordinate	1	0.445	0.44	[0.36, 0.53]
$x$ -coordinate	2	0.395	0.40	[0.34, 0.46]
$y$ -coordinate	2	0.46	0.46	[0.36, 0.57]
$x$ -coordinate	3	0.39	0.37	[0.30, 0.44]
$y$ -coordinate	3	0.39	0.41	[0.29, 0.53]
$x$ -coordinate	4	0.47	0.47	[0.39, 0.54]
$y$ -coordinate	4	0.39	0.38	[0.28, 0.47]
$x$ -coordinate	5	0.47	0.47	[0.40, 0.55]
$y$ -coordinate	5	0.235	0.27	[0.18, 0.36]
$x$ -coordinate	6	0.18	0.22	[0.13, 0.30]
$y$ -coordinate	6	0.455	0.49	[0.38, 0.60]

Table 3: Source estimates statistics summary.

<b>AE Source</b>	<b>PM for PF</b>	<b>PM for UKF</b>
1	0.0207	0.0390
2	0.0115	0.0679
3	0.0508	0.1458
4	0.0218	0.0569
5	0.0709	0.2705
6	0.1152	0.3404

Table 4: Comparison of performance of proposed algorithm versus UKF based Bayesian estimation algorithm. The metric  $PM$  is a relative error  $\ell_2$  norm.